Relativistic spin-polarized KKR theory for superconducting heterostructures: Oscillating order parameter in the Au layer of Nb/Au/Fe trilayers

Gábor Csire,[1,2] András Deák,[3] Bendegúz Nyári,[3] Hubert Ebert,[4] James F. Annett,[1] and Balázs Újfalussy[2]
[1]*H. H. Wills Physics Laboratory, University of Bristol, Tyndall Ave, BS8-1TL, United Kingdom*
[2]*Institute for Solid State Physics and Optics, Wigner Research Centre for Physics, Hungarian Academy of Sciences, P.O. Box 49, H-1525 Budapest, Hungary*
[3]*Department of Theoretical Physics, Budapest University of Technology and Economics, Budafoki út 8, H-1111 Budapest, Hungary*
[4]*Department Chemie/Phys. Chemie, Ludwig-Maximilians-Universität München, Germany*

(Received 22 November 2017; published 23 January 2018)

The fully relativistic spin-polarized multiple-scattering theory is developed for inhomogeneous superconductors, including superconducting/normal-metal/ferromagnet heterostructures. The method allows the solution of the first-principles Dirac–Bogoliubov–de Gennes equations combined with a semiphenomenological parametrization of the exchange-correlation functional. Simple conditions are derived for the case when the right-hand-side and left-hand-side solutions must be treated separately when setting up the corresponding Green's function. As an application of the theory, we calculate the order parameters of Nb/Fe and Nb/Au/Fe systems. We find Fulde-Ferrell-Larkin-Ovchinnikov-like oscillations in the iron layers, but more interestingly an oscillatory behavior is observed in the gold layers as well. The band-structure calculations suggest that this is the consequence of an interplay between the quantum-well states and ferromagnetism.

DOI: 10.1103/PhysRevB.97.024514

I. INTRODUCTION

More than five decades ago, Fulde and Ferrell [1] and Larkin and Ovchinnikov [2] (FFLO) demonstrated that, in a ferromagnetic superconductor at low temperature, the superconducting order parameter may change sign in real space. Superconducting/ferromagnet systems can exhibit a similar effect [3]; the order parameter extends from a superconductor to a ferromagnet with damped oscillatory behavior. This leads to many interesting effects, such as the oscillations of the critical current and the critical temperature, or the periodic transitions from the zero-phase to the π-phase state in superconductor/ferromagnet/superconductor (S/F/S) Josephson junctions, while varying the thickness of the ferromagnetic layer [4,5]. Practically, all interesting phenomena related to the interplay between superconductivity and magnetism or relativistic effects in S/F structures exist at the nanoscale range. The observation of these effects became possible in the last decade due to the development in the preparation of high-quality heterostructures [6,7]. Relativistic effects can also have great consequences on superconductivity. It has been known for a long time that spin-orbit coupling (SOC) can influence the symmetry of the order parameter [8] and Josephson currents [9]. However, its impact on noncentrosymmetric systems [10–12] and on the proximity effect [13–17] is getting more interest only recently, while it is also a key ingredient in possible realizations for Majorana fermions [18].

A logical step forward is to develop a relativistic spin-polarized microscopic theory for realistic materials which can treat relativistic effects and superconductivity together with spin and orbital magnetism on the same footing. The microscopic theory of inhomogeneous superconductors is based on the Bogoliubov–de Gennes (BdG) equations [19]. The relativistic generalization of this theory—called Dirac–Bogoliubov–de Gennes (DBdG) equations—was established by Capelle and Gross [20,21]. To be able to treat arbitrary geometries including semi-infinite geometries without the use of a giant supercell, in this paper we develop a relativistic spin-polarized screened Korringa-Kohn-Rostoker (KKR) method [22–31] for the solution of the DBdG equations. The KKR method was proven to be a very powerful tool over the last decade with a very broad range of possible applications (including impurities, disordered systems, magnetic response functions, magnetic anisotropy, pair interaction parameters, transport quantities, spectroscopy, etc.). A review about such applications can be found in Ref. [30]. In Ref. [32] the KKR method has been extended for the solution of the BdG equations. In the present paper we provide the generalization of the screened-KKR method for the solution of the Dirac–Bogoliubov–de Gennes equations.

The theoretical formalism is developed in Sec. II. In Sec. III the method is applied for Nb/Fe and Nb/Au/Fe heterostructures. For Nb/Au/Fe heterostructures, Yamazaki *et al.* [6,7] have found long-period oscillations in the critical temperature as a function of the gold thickness. Interestingly, none of the models based on Ruderman-Kittel-Kasuya-Yoshida coupling, Friedel oscillations, and FFLO oscillations (in the iron layers) were able to solve the puzzle behind the observed oscillatory behavior of T_c. Recent neutron reflectivity measurements [33] also suggest an oscillating behavior for the order parameter in the Au layers. In the present paper we provide a possible explanation for this phenomenon based on the properties of the band structure, and on the solution of the DBdG equations. Finally, Sec. IV is devoted to a summary and conclusions.

II. THE DBDG-SKKR METHOD

In this section we generalize the screened-KKR method for the solution of the Dirac–Bogoliubov–de Gennes equations assuming a pointlike s-wave interaction for the pairing. The method allows the calculation of the Green's function for layered systems, which contains all information about the ground state, and hence makes it unnecessary to obtain the Kohn-Sham orbitals.

A. First-principles DBdG equations

Capelle and Gross [20] showed that in the relativistic case, 16 different order parameters exist with different symmetry properties (these order parameters are 4×4 matrices). However, a symmetry analysis with respect to the Lorentz group results in only five different types of order parameters that are consistent with the requirement of covariance (in the nonrelativistic case there are different types of order parameters, which describe singlet and triplet superconductivity). In the nonrelativistic BCS theory pairing occurs between electrons of opposite spin and opposite momentum, thus, for spin singlet pairing the key symmetry is time-reversal invariance. This property should be kept in the relativistic case, hence, one can identify the time-reversal matrix $\boldsymbol{\eta}$ (which is one of the 16 order parameters) as the relativistic version of the BCS order parameter. Therefore, the relativistic order parameter—with assuming a contact potential for the interaction—is given by

$$\chi(\vec{r}) = \langle \Psi^T(\vec{r}) \boldsymbol{\eta} \Psi(\vec{r}) \rangle, \tag{1}$$

with the time-reversal matrix

$$\boldsymbol{\eta} = \begin{pmatrix} 0 & 1 & 0 & 0 \\ -1 & 0 & 0 & 0 \\ 0 & 0 & 0 & 1 \\ 0 & 0 & -1 & 0 \end{pmatrix}, \tag{2}$$

and $\Psi(\vec{r})$ represents the four-component Dirac spinor field operator. The proper relativistic generalization leads to the following DBdG Hamiltonian written in Rydberg units ($\hbar = 1$, $m = 1/2$, $e^2 = 2$):

$$H_{\mathrm{DBdG}} = \begin{pmatrix} H_D & D_{\mathrm{eff}}(\vec{r})\boldsymbol{\eta} \\ D^*_{\mathrm{eff}}(\vec{r})\boldsymbol{\eta}^T & -H^*_D \end{pmatrix}, \tag{3}$$

where

$$H_D = c\boldsymbol{\alpha}\mathbf{p} + (\boldsymbol{\beta} - \mathbb{I}_4)c^2/2 + [V_{\mathrm{eff}}(\vec{r}) - E_F]\mathbb{I}_4 + \boldsymbol{\Sigma}\vec{B}_{\mathrm{eff}}(\vec{r}) + e\boldsymbol{\alpha}\vec{A}(\vec{r}), \tag{4}$$

$$\boldsymbol{\alpha} = \begin{pmatrix} 0 & \boldsymbol{\sigma} \\ \boldsymbol{\sigma} & 0 \end{pmatrix}, \quad \boldsymbol{\beta} = \begin{pmatrix} \mathbb{I}_2 & 0 \\ 0 & -\mathbb{I}_2 \end{pmatrix}, \quad \boldsymbol{\Sigma} = \begin{pmatrix} \boldsymbol{\sigma} & 0 \\ 0 & \boldsymbol{\sigma} \end{pmatrix}, \tag{5}$$

and $\boldsymbol{\sigma}$ denotes the Pauli matrices. By adopting the simple semiphenomenological parametrization of the exchange-correlation functional described in Refs. [32,34,35], the effective electrostatic potential, exchange field, and pairing potential can be written as

$$V_{\mathrm{eff}}(\vec{r}) = V_{\mathrm{ext}}(\vec{r}) + \int \frac{\rho(\vec{r}')}{|\vec{r} - \vec{r}'|} d^3r' + \frac{\delta E^0_{\mathrm{xc}}[\rho,\vec{m}]}{\delta\rho(\vec{r})}, \tag{6a}$$

$$\vec{B}_{\mathrm{eff}}(\vec{r}) = \vec{B}_{\mathrm{ext}}(\vec{r}) + \frac{\delta E^0_{\mathrm{xc}}[\rho,\vec{m}]}{\delta m(\vec{r})}, \tag{6b}$$

$$D_{\mathrm{eff}}(\vec{r}) = \Lambda\chi(\vec{r}), \tag{6c}$$

where Λ is the strength of the interaction responsible for superconductivity (which can be treated as an adjustable semiphenomenological parameter), $V_{\mathrm{ext}}(\vec{r})$ is the external potential (e.g., the Coulomb attraction from the protons), $\vec{B}_{\mathrm{ext}}(\vec{r})$ is the external field, $\rho(\vec{r})$ is the charge density, $\vec{m}(\vec{r})$ is the magnetization density, and $E^0_{\mathrm{xc}}[\rho,\vec{m}]$ is the usual (local spin density approximation) exchange-correlation energy for normal electrons. For the sake of completeness we mention that a nonrelativistic spin density functional theory for superconductors and the approximated exchange-correlation functionals have been developed by Linscheid *et al.* [36,37]. At present, this is the most accurate theory, which allows the first-principles calculation of the superconducting transition temperature for bulk systems [38–45]. However, despite the simplicity of this approximation, it was able to describe many features of bulk niobium [34] and the proximity effect in Nb/Au heterostructures [35,46].

B. Generalized screened-KKR method

During the generalization of the KKR method for the solution of the DBdG equations, we follow the footsteps of Refs. [31,47] and describe the key differences compared to the normal state. In the KKR method, the potential will be treated in the so-called muffin-tin approximation, i.e., the potential is written as a sum of single-domain potentials centered around each lattice site, n, namely, $V_{\mathrm{eff}}(\vec{r}) = \sum_n V_n(r)$, $B_{\mathrm{eff}}(\vec{r}) = \sum_n B_n(r)$, $D_{\mathrm{eff}}(\vec{r}) = \sum_n D_n(r)$. The potentials are muffin-tin type, which means that they are zero if $r = |\vec{r}_n| \geqslant S_n$, where S_n is the muffin-tin radius.

Compared to the nonrelativistic KKR theory, the relativistic version leads to a number of technical complications, especially, the need to distinguish between the right- (RHS) and the left-hand-side solutions (LHS) of the DBdG equations. The RHS $\psi(z)$ (eight-component function) is defined as

$$(z - H_{\mathrm{DBdG}})|\Psi(z)\rangle = 0 \tag{7}$$

and the corresponding LHS $\langle\Psi^\times(z)|$ can be written as

$$\langle\Psi^\times(z)|(z - H_{\mathrm{DBdG}}) = 0. \tag{8}$$

The resolvent of the DBdG Hamiltonian can be defined as

$$\mathcal{G}(z) = (z\mathbb{I} - H_{\mathrm{DBdG}})^{-1}, \tag{9}$$

which has the usual property

$$\mathcal{G}(z^*) = \mathcal{G}(z)^\dagger. \tag{10}$$

As was shown for the nonrelativistic case, the Green's function can be given also for the relativistic case in terms of the spectral representation:

$$G^{ab}(z,\vec{r},\vec{r}\,') = \sum_n \frac{\psi^a_n(z,\vec{r})\left[\phi^b_n(z,\vec{r}\,')\right]^\dagger}{z - E_n(z)}, \tag{11}$$

where the right- and left-hand-side solutions, $\psi^a_n(z,\vec{r})$ and $\phi^b_n(z,\vec{r})$, respectively, are four-component functions, and a,b refer to the electron-hole index.

A quantum state in the nonrelativistic case is fully determined by the quantum numbers $L = (l,m)$, while in the relativistic case we search the RHS solutions of the DBdG

equations in the following form:

$$\Psi(z,\vec{r}) = \sum_{Q} \begin{pmatrix} g^{e}_{Q}(z,r)\chi_{Q}(\hat{r}) \\ i f^{e}_{Q}(z,r)\chi_{\overline{Q}}(\hat{r}) \\ g^{h}_{Q}(z,r)\chi^{*}_{Q}(\hat{r}) \\ -i f^{h}_{Q}(z,r)\chi^{*}_{\overline{Q}}(\hat{r}) \end{pmatrix}, \tag{12}$$

where $Q = (\kappa,\mu)$ and $\overline{Q} = (-\kappa,\mu)$ are the composite indices for the spin-orbit (κ) and magnetic (μ) quantum numbers; $g^{e(h)}_{Q}(z,r)$ and $f^{e(h)}_{Q}(z,r)$ are the large and small components of the electron (hole) part of the solution, respectively. The spin-angular function is an eigenfunction of the spin-orbit operator $K = \boldsymbol{\sigma} L + \mathbb{I}$,

$$K|\kappa\mu\rangle = -\kappa|\kappa\mu\rangle. \tag{13}$$

This basis set has the advantage that the corresponding matrix of the spin-orbit operator is diagonal. However, since the magnetic part of the Hamiltonian does not commute with the total angular momentum operator, it will introduce couplings between states with different κ,μ quantum numbers. For later purposes, the following notations are also introduced: $\bar{l} = l - S_k$, and $S_k = \kappa/|\kappa|$ the sign of κ.

With integration over the angular parts and using the orthonormality of the Clebsch-Gordan coefficients and the following results [28]

$$-i\sigma_y \chi^{*}_{\kappa\mu}(\hat{r}) = (-1)^{\mu+1/2} S_\kappa \chi_{\kappa-\mu}(\hat{r}), \tag{14}$$

the radial DBdG equations for arbitrary magnetic field can be written as

$$\begin{pmatrix} z+E_F & c\left(\frac{d}{dr}+\frac{1}{r}-\frac{\kappa}{r}\right) & 0 & 0 \\ c\left(\frac{d}{dr}+\frac{1}{r}+\frac{\kappa}{r}\right) & z+E_F+c^2 & 0 & 0 \\ 0 & 0 & E_F-z & c\left(\frac{d}{dr}+\frac{1}{r}-\frac{\kappa}{r}\right) \\ 0 & 0 & c\left(\frac{d}{dr}+\frac{1}{r}+\frac{\kappa}{r}\right) & -z+E_F+c^2 \end{pmatrix} \begin{pmatrix} g^{e}_{Q}(z,r) \\ f^{e}_{Q}(z,r) \\ g^{h}_{Q}(z,r) \\ f^{h}_{Q}(z,r) \end{pmatrix}$$
$$= \sum_{Q'} \begin{pmatrix} u^{++}_{QQ'}(r) & i u^{+-}_{QQ'}(r) & \Delta_{QQ'}(r) & 0 \\ -i u^{-+}_{QQ'}(r) & u^{--}_{QQ'}(r) & 0 & \Delta_{QQ'}(r) \\ \Delta^{*}_{QQ'}(r) & 0 & u^{++}_{QQ'}(r)^{*} & -i u^{+-}_{QQ'}(r)^{*} \\ 0 & \Delta^{*}_{QQ'}(r) & i u^{-+}_{QQ'}(r)^{*} & u^{--}_{QQ'}(r)^{*} \end{pmatrix} \begin{pmatrix} g^{e}_{Q'}(z,r) \\ f^{e}_{Q'}(z,r) \\ g^{h}_{Q'}(z,r) \\ f^{h}_{Q'}(z,r) \end{pmatrix}, \tag{15}$$

where

$$u^{++}_{QQ'}(r) = V(r) + \sum_{i=x,y,z} \langle \chi_Q | \sigma_i B_i(r) | \chi_{Q'} \rangle, \tag{16}$$

$$u^{+-}_{QQ'}(r) = \sum_{i=x,y,z} \langle \chi_Q | e\sigma_i A_i(r) | \chi_{\overline{Q}'} \rangle, \tag{17}$$

$$u^{-+}_{QQ'}(r) = \sum_{i=x,y,z} \langle \chi_{\overline{Q}'} | e\sigma_i A_i(r) | \chi_{Q'} \rangle, \tag{18}$$

$$u^{--}_{QQ'}(r) = V(r) - \sum_{i=x,y,z} \langle \chi_{\overline{Q}} | \sigma_i B_i(r) | \chi_{\overline{Q}'} \rangle, \tag{19}$$

$$\Delta_{QQ'}(r) = (-1)^{\mu'-1/2} S_{\kappa'} \delta_{\kappa\kappa'} \delta_{\mu-\mu'} D(r). \tag{20}$$

The last definition for the pairing potential matrix shows that the pairing interaction couples electrons with κ,μ quantum numbers to holes with κ, $-\mu$ quantum numbers. This is the direct consequence of our initial assumption that the pairing acts between Kramers pairs, namely, between electrons and their time-reversed pairs (holes). If no magnetic field is present, the LHS solutions can also be obtained by acting the time-reversal operator on the RHS solutions as was pointed out by Tamura [28]. It should also be emphasized that with an appropriate semiphenomenological parametrization of the exchange-correlation functional the method could be applied for unconventional superconductors assuming interaction between different orbitals as was done in Ref. [48]. These parameters may be identified by fitting an appropriate number of experiments. Then in a next step we can predict the outcome of other experiments without additional adjustable parameters.

The ansatz for the LHS solution

$$\Psi^{\times}(z,\vec{r}) = \sum_{Q} \begin{pmatrix} g^{e\times}_{Q}(z,r)\chi^{\dagger}_{Q}(\hat{r}) \\ -i f^{e\times}_{Q}(z,r)\chi^{\dagger}_{\overline{Q}}(\hat{r}) \\ g^{h\times}_{Q}(z,r)\chi^{T}_{Q}(\hat{r}) \\ i f^{h\times}_{Q}(z,r)\chi^{T}_{\overline{Q}}(\hat{r}) \end{pmatrix}^{T}, \tag{21}$$

leads to the equation

$$\begin{pmatrix} z+E_F & c\left(\frac{d}{dr}+\frac{1}{r}-\frac{\kappa}{r}\right) & 0 & 0 \\ c\left(\frac{d}{dr}+\frac{1}{r}+\frac{\kappa}{r}\right) & z+E_F+c^2 & 0 & 0 \\ 0 & 0 & E_F-z & c\left(\frac{d}{dr}+\frac{1}{r}-\frac{\kappa}{r}\right) \\ 0 & 0 & c\left(\frac{d}{dr}+\frac{1}{r}+\frac{\kappa}{r}\right) & -z+E_F+c^2 \end{pmatrix} \begin{pmatrix} g^{e\times}_Q(z,r) \\ f^{e\times}_Q(z,r) \\ g^{h\times}_Q(z,r) \\ f^{h\times}_Q(z,r) \end{pmatrix}$$
$$= \sum_{Q'} \begin{pmatrix} u^{++}_{Q'Q}(r) & -iu^{+-}_{Q'Q}(r) & \Delta^*_{QQ'}(r) & 0 \\ iu^{-+}_{Q'Q}(r) & u^{--}_{Q'Q}(r) & 0 & \Delta^*_{QQ'}(r) \\ \Delta_{QQ'}(r) & 0 & u^{++}_{Q'Q'}(r)^* & iu^{+-}_{Q'Q}(r)^* \\ 0 & \Delta_{QQ'}(r) & -iu^{-+}_{Q'Q}(r)^* & u^{--}_{Q'Q}(r)^* \end{pmatrix} \begin{pmatrix} g^{e\times}_{Q'}(z,r) \\ f^{e\times}_{Q'}(z,r) \\ g^{h\times}_{Q'}(z,r) \\ f^{h\times}_{Q'}(z,r) \end{pmatrix}. \tag{22}$$

Therefore, the LHS can be obtained from the RHS by substituting

$$D(r) \to D^*(r),$$
$$u^{\pm\mp}_{Q'Q}(r) \to -u^{\mp\pm}_{QQ'}(r),$$
$$u^{\pm\pm}_{Q'Q}(r) \to u^{\pm\pm}_{QQ'}(r),$$

which also means that the RHS solution is the same as the LHS solution only if

$$D(r) = D^*(r), \tag{23}$$

$$u^{\pm\mp}_{Q'Q}(r) = -u^{\mp\pm}_{QQ'}(r), \tag{24}$$

$$u^{\pm\pm}_{Q'Q}(r) = u^{\pm\pm}_{QQ'}(r). \tag{25}$$

Physically, the last condition means that the magnetic field should have x and z components only. In principle, the vectors $\vec{B}(\vec{r})$ and $\vec{A}(\vec{r})$ can be rotated to a local frame, which points along the $\hat{z}$ direction as is usually done. In the normal state it has two advantages: the least amount of coupling occurs between the states with different κ,μ quantum numbers, and there is no need to distinguish the LHS and RHS solutions. However, these conditions show that even if the magnetic field points along $\hat{z}$, the LHS and RHS solutions can still be different for a complex pairing potential, which has important consequences, for example, in Josephson junctions.

In practice, we solve the RHS and LHS DBdG equations in the global frame with a predictor-corrector algorithm on logarithmic scale similarly as was done for the radial scalar relativistic BdG equations in Ref. [32].

Following the footsteps of Ref. [47], the free-particle Green's function can be derived from the nonrelativistic one, which leads to

$$G^{ab}_0(z,\vec{r},\vec{r}\,') = -ip^a\delta_{ab}\sum_Q \big[j^a_Q(z,\vec{r}) h^a_Q(z,\vec{r}\,')^\times \theta(r'-r) + h^a_Q(z,\vec{r}) j^a_Q(z,\vec{r}\,')^\times \theta(r-r')\big], \tag{26}$$

where

$$p^{e(h)} = \sqrt{(E_F \pm z)\left(1+\frac{E_F \pm z}{c^2}\right)} \tag{27}$$

and the relativistic forms of the Bessel and outgoing (Im $p^e > 0$) Hankel functions for the electron-type states are defined as

$$j^e_Q(z,\vec{r}) = \begin{pmatrix} j_l(p^e r)\chi_Q(\hat{r}) \\ \frac{iS_k p^e c}{z+E_F+c^2/2} j_{\bar{l}}(p^e r)\chi_{\bar{Q}}(\hat{r}) \end{pmatrix}, \tag{28}$$

$$j^{e\times}_Q(z,\vec{r}) = \begin{pmatrix} j_l(p^e r)\chi^\dagger_Q(\hat{r}) \\ \frac{-iS_k p^e c}{z+E_F+c^2/2} j_{\bar{l}}(p^e r)\chi^\dagger_{\bar{Q}}(\hat{r}) \end{pmatrix}^T, \tag{29}$$

$$h^e_Q(z,\vec{r}) = \begin{pmatrix} h^+_l(p^e r)\chi_Q(\hat{r}) \\ \frac{iS_k p^e c}{z+E_F+c^2/2} h^+_{\bar{l}}(p^e r)\chi_{\bar{Q}}(\hat{r}) \end{pmatrix}, \tag{30}$$

$$h^{e\times}_Q(z,\vec{r}) = \begin{pmatrix} h^+_l(p^e r)\chi^\dagger_Q(\hat{r}) \\ \frac{-iS_k p^e c}{z+E_F+c^2/2} h^+_{\bar{l}}(p^e r)\chi^\dagger_{\bar{Q}}(\hat{r}) \end{pmatrix}^T, \tag{31}$$

and for hole-type states (Im $p^h > 0$)

$$j^h_Q(z,\vec{r}) = \begin{pmatrix} j_l(p^h r)\chi^*_Q(\hat{r}) \\ \frac{-iS_k p^h c}{-z+E_F+c^2/2} j_{\bar{l}}(p^h r)\chi^*_{\bar{Q}}(\hat{r}) \end{pmatrix}, \tag{32}$$

$$j^{h\times}_Q(z,\vec{r}) = \begin{pmatrix} j_l(p^h r)\chi^T_Q(\hat{r}) \\ \frac{iS_k p^h c}{-z+E_F+c^2/2} j_{\bar{l}}(p^h r)\chi^T_{\bar{Q}}(\hat{r}) \end{pmatrix}^T, \tag{33}$$

$$h^h_Q(z,\vec{r}) = \begin{pmatrix} -h^+_l(p^h r)\chi^*_Q(\hat{r}) \\ \frac{iS_k p^h c}{-z+E_F+c^2/2} h^+_{\bar{l}}(p^h r)\chi^*_{\bar{Q}}(\hat{r}) \end{pmatrix}, \tag{34}$$

$$h^{h\times}_Q(z,\vec{r}) = \begin{pmatrix} -h^+_l(p^h r)\chi^T_Q(\hat{r}) \\ \frac{-iS_k p^h c}{-z+E_F+c^2/2} h^+_{\bar{l}}(p^h r)\chi^T_{\bar{Q}}(\hat{r}) \end{pmatrix}^T. \tag{35}$$

Similarly, as was described in Ref. [47], the relativistic real-space electronic structure constant should be derived from the nonrelativistic structure constant $G^{ee,\mathrm{nrel},nm}_{0,LL'}(z)$ by transforming it into the $|\kappa\mu\rangle$ basis, while the hole part of the relativistic structure constant can be constructed in the $|\kappa\mu\rangle^*$ basis using the nonrelativistic formula [32] $G^{hh,\mathrm{nrel},nm}_{0,LL'}(z) = -G^{ee,\mathrm{nrel},nm}_{0,LL'}(-z)$.

The following supermatrix formalism can be introduced for the scattering matrices, the matrices of the structure constant, and the scattering path operator:

$$\mathbf{t}(z) = \left\{t^{n,ab}_{QQ'}(z)\delta_{nm}\right\}, \tag{36}$$

$$\mathbf{G}_0(z) = \left\{G^{nm,ab}_{0,QQ'}(z)(1-\delta_{nm})\delta_{ab}\right\}, \tag{37}$$

$$\boldsymbol{\tau}(z) = \left\{\tau^{nm,ab}_{QQ'}(z)\right\}, \tag{38}$$

where $\boldsymbol{\tau}(z)$ can be determined from the single-site t matrix and the real-space structure constant similarly to normal state in the supermatrix formalism

$$\boldsymbol{\tau}(z) = [\mathbf{t}(z)^{-1} - \mathbf{G}_0(z)]^{-1}. \tag{39}$$

Based on the analogy between the expansions of the free-particle Green's function in the nonrelativistic case, and in the relativistic case, the derivation of the one-particle Green's function in the relativistic case is straightforward and leads to the following formula:

$$\begin{aligned}\mathbf{G}(z,\vec{r},\vec{r}\,') = &\sum_{QQ'} \mathbf{Z}_Q(z,\vec{r})\boldsymbol{\tau}_{QQ'}(z)\mathbf{Z}_{Q'}(z,\vec{r}')^{\times} \\ &- \theta(r'-r)\sum_{Q} \mathbf{Z}_Q(z,\vec{r})\mathbf{J}_Q(z,\vec{r}')^{\times} \\ &- \theta(r-r')\sum_{Q} \mathbf{J}_Q(z,\vec{r})\mathbf{Z}_Q(z,\vec{r}')^{\times}, \end{aligned} \tag{40}$$

where $\mathbf{J}_Q, \mathbf{J}_Q^{\times}, \mathbf{Z}_Q, \mathbf{Z}_Q^{\times}$ (matrices in electron-hole indices) represent the irregular RHS, irregular LHS, regular RHS, and regular LHS solutions of the DBdG equations inside the muffin-tin spheres, respectively, and they have the following asymptotic behavior for $r > S_n$:

$$J_Q^{ab}(z,r) = j_Q^a(z,r)\delta_{ab}, \tag{41a}$$

$$J_Q^{ab}(z,r)^{\times} = j_Q^a(z,r)^{\times}\delta_{ab}, \tag{41b}$$

$$Z_Q^{ab}(z,r) = \sum_{Q'} j_{Q'}^a(z,r)m_{Q'Q}^{ab}(z) - ip^a h_Q^a(z,r)\delta_{ab}, \tag{41c}$$

$$Z_Q^{ab}(z,r)^{\times} = \sum_{Q'} m_{QQ'}^{ab}(z) j_{Q'}^b(z,r)^{\times} - ip^a h_Q^a(z,r)^{\times}\delta_{ab}, \tag{41d}$$

where we introduced the inverse t matrix $m_{QQ'}^{ab}(z) = [\underline{t}^{-1}(z)]_{QQ'}^{ab}$. Here, it should be emphasized that the formal structure of the Green's function is not changed compared to the nonrelativistic and also the nonsuperconducting case. Importantly, the scheme presented in Ref. [49] will also allow us to manipulate the spin-orbit coupling in calculations.

The above expressions can be applied to surfaces and interfaces straightforwardly following the recipe of the screened-KKR (SKKR) formalism introduced in Refs. [25,26], where the two-dimensional (2D) periodicity of the layers is introduced by the 2D lattice Fourier transformed version of the real-space structure constant. To obtain structure constants that are localized in real space, a special reference system (uniform distribution of constant repulsive potentials) is used instead of free space. This gets manifested in a screening transformation on the structure constant. In the supermatrix formalism we used above, this screening transformation can be written in a way that is formally equivalent to the description in Sec. III of Ref. [25].

For layered systems, similarly to the nonrelativistic case, the anomalous density $\chi_I(\vec{r})$ can be obtained for layer I from the 2D lattice Fourier transformed version of the anomalous part of the Green's function. In particular, the singlet order parameter could be derived from the Green's function obtained in the $|\kappa\mu\rangle$ basis as follows:

$$\begin{aligned}\mathrm{Re}\,\chi_I(\vec{r}) = &-\frac{1}{2\pi}\int_{-\infty}^{\infty} d\varepsilon \int_{\mathrm{BZ}} d^2k_{\parallel}[1-2f(\varepsilon)] \\ &\times \mathrm{Im}\,\mathrm{Tr}_Q \boldsymbol{\eta} G^{eh,\mathrm{II}}(\varepsilon + i0,\vec{r},\vec{k}_{\parallel}) \\ &- \frac{1}{2\pi}\int_{-\infty}^{\infty} d\varepsilon \int_{\mathrm{BZ}} d^2k_{\parallel}[1-2f(\varepsilon)] \\ &\times \mathrm{Im}\,\mathrm{Tr}_Q \boldsymbol{\eta} G^{he,\mathrm{II}}(\varepsilon + i0,\vec{r},\vec{k}_{\parallel}), \end{aligned} \tag{42}$$

$$\begin{aligned}\mathrm{Im}\,\chi_I(\vec{r}) = &\frac{1}{2\pi}\int_{-\infty}^{\infty} d\varepsilon \int_{\mathrm{BZ}} d^2k_{\parallel}[1-2f(\varepsilon)] \\ &\times \mathrm{Re}\,\mathrm{Tr}_Q \boldsymbol{\eta} G^{eh,\mathrm{II}}(\varepsilon + i0,\vec{r},\vec{k}_{\parallel}) \\ &- \frac{1}{2\pi}\int_{-\infty}^{\infty} d\varepsilon \int_{\mathrm{BZ}} d^2k_{\parallel}[1-2f(\varepsilon)] \\ &\times \mathrm{Re}\,\mathrm{Tr}_Q \boldsymbol{\eta} G^{he,\mathrm{II}}(\varepsilon + i0,\vec{r},\vec{k}_{\parallel}). \end{aligned} \tag{43}$$

III. RESULTS

A. Nb/Fe bcc(001)

The experimental study of the interplay between superconductivity and magnetism has been carried out for many S/F combinations, especially for Nb/Fe systems [6,7,50–52]. Hence, we apply the theory to study the system of Fe overlayers on Nb(001) with assuming exchange field in the z direction. For the Nb, we used the experimental lattice constant of 3.3 Å in the bcc structure, which consequently leads to the two-dimensional lattice constant 3.3 Å in the (001) direction throughout the whole system.

The self-consistent electrostatic and exchange potentials, and work functions for the DBdG calculations were obtained from the normal-state relativistic calculations. The self-consistent calculations were performed for systems containing a semi-infinite Nb, and in the interface region there were an additional six Nb layers and subsequently various numbers of Fe layers (up to 12 layers), three vacuum layers, followed by a semi-infinite vacuum. In Fig. 1 we show the layer dependence of the electronic structure [namely, the layer-dependent contour plot of the Bloch spectral function (BSF)] in an (ℓ,m,s) representation which can be obtained from the (κ,μ) representation we used throughout the derivations in the previous section by a Clebsch-Gordan transformation. In the iron the majority spin states are in the spin-up channel at the Fermi level as shown in Fig. 2, and the signatures of confinement can be observed in the spin-down channel leading to quantum-well states. Compared to Nb, the density of states (DOS) is much larger for the spin-up electrons and much smaller for the spin-down electrons. Where the DOS in the bulk Nb is low, the spin-down states in the Fe are confined, and they cannot scatter into the Nb, while on the other side the system is limited by vacuum. In regions where the DOS is high in the Nb, the spin-down states in the Fe are smeared out, since these states can scatter more easily into the other side of the interface. The proximity also induces magnetism in the Nb layers, which is quite significant for the interface Nb layer showing an induced magnetic moment of $0.4\mu B$.

To investigate what happens when the Nb is in the superconducting state and a thin ferromagnetic iron layer is

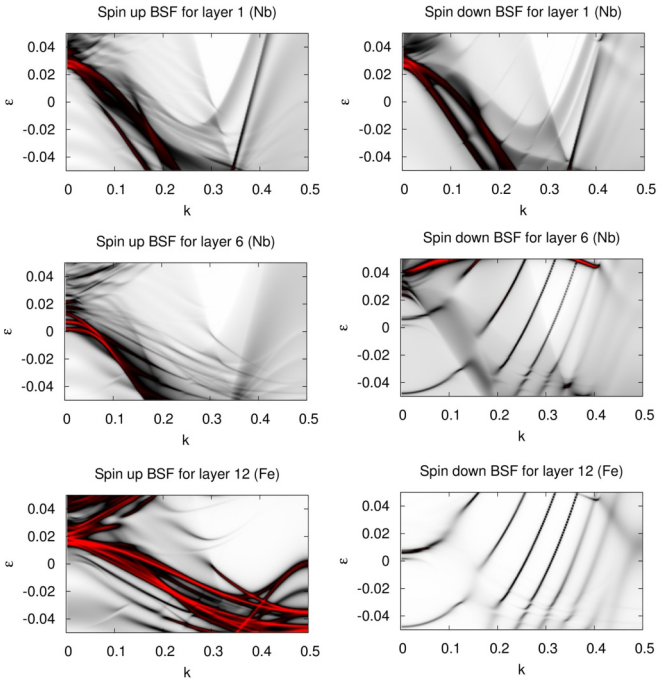

FIG. 1. Contour plot of the BSF (normal-state band structure) for different layers in the $k_x = k_y$ direction. In the interface region there are 6 Nb layers, 12 Fe layers, and 3 vacuum layers.

placed in contact with it, we use a semiphenomenological parametrization of the electron-phonon coupling. Namely, we choose the electron-phonon coupling in the Nb to reproduce the experimental value of the gap (0.2 mRy) in the bulk Nb [53]. This leads to $\Lambda = 0.11$ eV, which was also obtained from the linear muffin-tin orbital method by Suvasini *et al.* [34]. We use this value for all Nb layers, and zero electron-phonon coupling is assumed for the Fe layers. For this situation the quasiparticle DOS was calculated from the solution of the DBdG equations shown in the bottom panel of Fig. 2. In the the same spin channel the holelike states can be obtained from the electronic ones by mirroring them to the Fermi energy. This property holds for not just the Nb layers, but also for the Fe layers as well. This is the consequence of the electron-hole symmetry of the nonrelativistic spin-generalized BdG equations as discussed in Ref. [54]. In accordance with experimental findings [55], an induced gap could not be observed in the BSF of the iron layers. The states in the iron extend into the Nb; however, their contributions to the full DOS can be neglected.

As was shown in Ref. [3], a Cooper pair entering into a ferromagnetic region results in acquiring a center-of-mass momentum, which leads to a spatial modulation of the order parameter: it exhibits a damping oscillatory behavior with its sign changing. This effect is very similar to the well-known FFLO state, where Cooper pairs with a nonzero center-of-mass moment result in an inhomogeneous order parameter. In our case the order parameter is obtained from the anomalous density as

$$\overline{\chi}_I = \frac{\int_{\Omega_{WS}} dr|\chi_I(r)|}{\int_{\Omega_{WS}} dr|\chi_{\text{Bulk}}(r)|}, \tag{44}$$

which in turn is calculated from the self-consistent solution of the DBdG equations. In Fig. 3 we show the order parameters

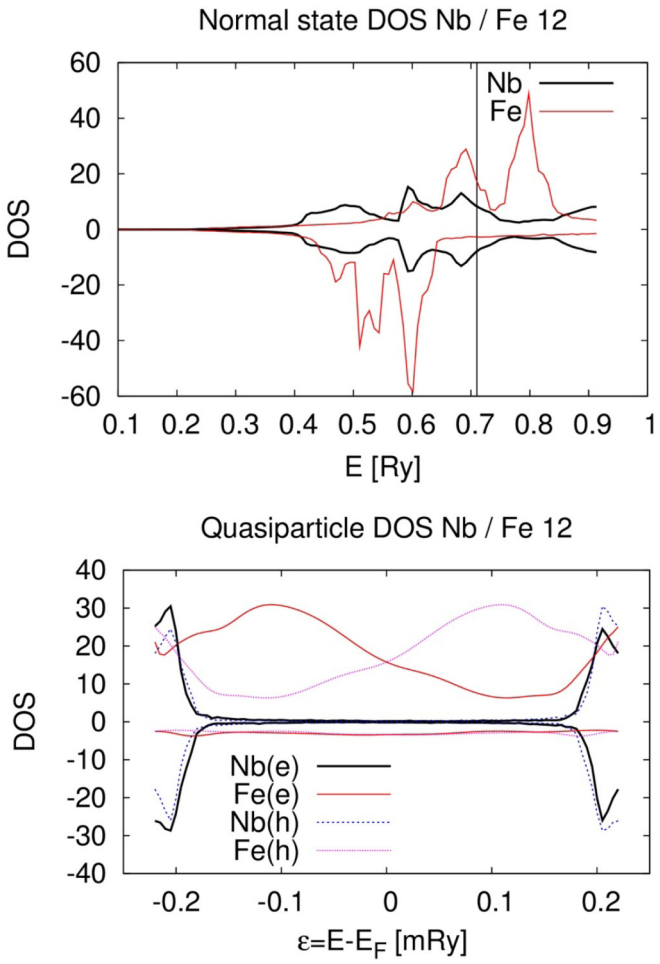

FIG. 2. Spin-resolved DOS and quasiparticle DOS for the Nb/Fe(001) system with 12 iron overlayers. The up-spin channel is indicated by positive, while the down-spin channel by negative values. The vertical line refers to the Fermi level. The curves correspond to the first Nb layer and an iron layer from the middle.

for the system with 12 Fe layers where the FFLO-type oscillations of the order parameter could be observed. As was shown in Refs. [5,56] these oscillations can lead to a

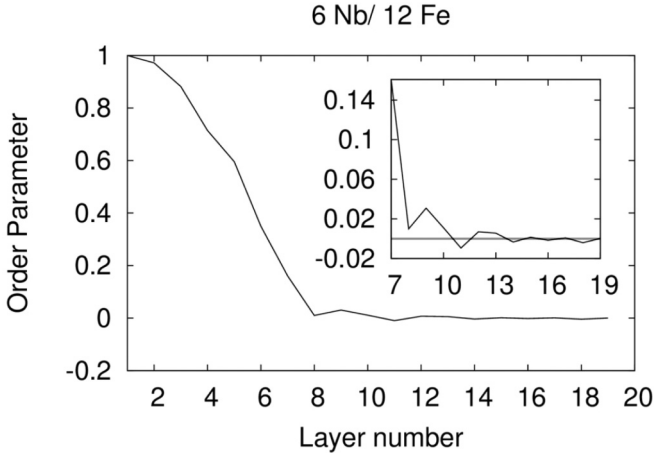

FIG. 3. Order parameter for the Nb/Fe(001) system with 12 iron overlayers. The inset shows the order parameter in the iron layers.

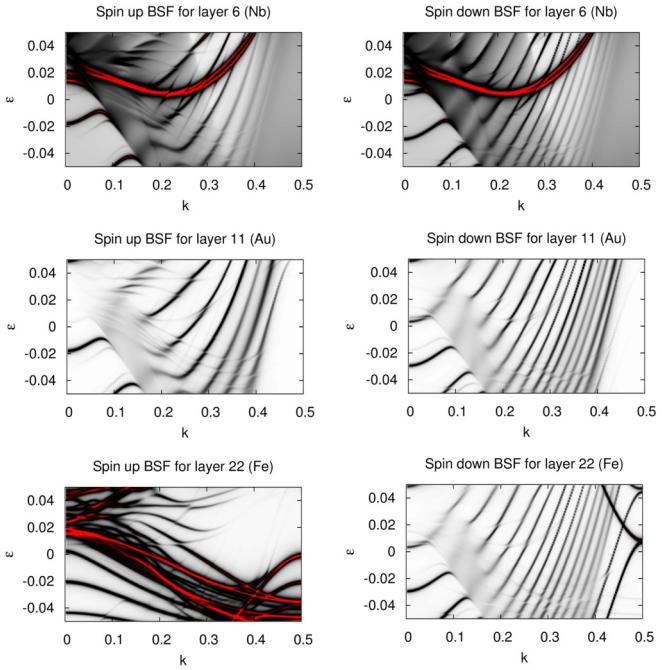

FIG. 4. Contour plot of the BSF (normal-state band structure) for different layers in the $k_x = k_y$ direction. In the interface region there are 6 Nb layers, 9 Au layers, 12 Fe layers, and 3 vacuum layers.

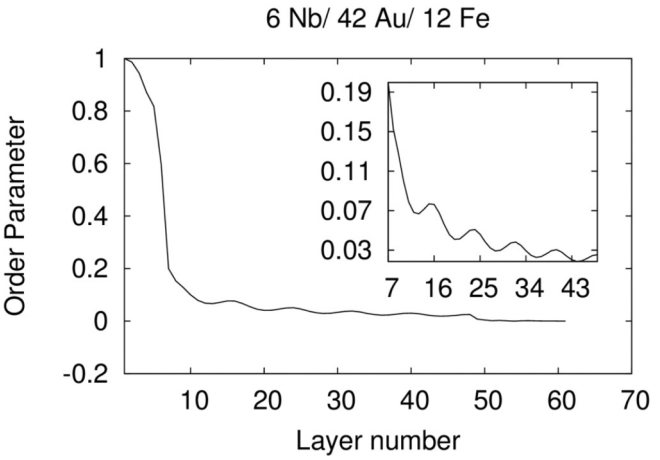

FIG. 5. Order parameter for the Nb/Au/Fe(001) system with 42 gold and 12 Fe overlayers. The inset shows the order parameter in the gold layers. The order shows an oscillating behavior with a period of eight layers.

nonmonotic behavior of the critical temperature (as a function of the iron thickness).

In principle, the presence of spin-orbit scattering could cause the spin singlet Cooper-pair wave function decaying to a spin triplet, and it could mix the Cooper pair with its spin-exchanged counterpartner (causes a pair to experience an exchange field which decreases the average field, therefore increasing the period of the order-parameter oscillations). However, while making calculations for the SOC=0 case we could not find any significant difference compared to the fully relativistic solution. Hence, we may conclude that the spin-orbit coupling in iron is not strong enough to have a measurable impact on the superconducting properties.

B. Nb/Au/Fe

We placed different numbers of Au layers (up to 42) between the Nb and Fe layers, where a fcc growth is assumed for the Au overlayers. While the results show that the Au layers remained nonmagnetic, spin-polarized bands around the Fermi level can be observed as shown in Fig. 4. This is the consequence of the different confinement for the spin-up and spin-down electrons. In fact, quantum-well states are splittings of the band of single-electron states into a series of subbands (caused by the quantization of the electron motion) which depends on the thickness of confinement. As Fig. 4 suggests, the spin-up electrons are confined in the Au layers only, while the spin-down electrons experience a confinement in both the Au and Fe layers. Therefore, due to the different confinement lengths between the spin channels, more bands are observed for the spin-up states than for the spin-down states. Calculations were for various directions of the exchange field; however, we found that they all lead to a very similar behavior, only the very fine details of the band structure change around the Fermi energy. Since the order parameter is influenced mostly by the states in close vicinity of the Fermi level, we can conclude that a pairing state (in the Au) can occur between two electrons on the induced split parts of the Fermi surface caused by the quantum-well states. Hence, the Cooper pair can acquire a finite momentum leading to the oscillation of the order parameter (analogously to the FFLO state). While SOC in Au is rather strong, it does not have a significant effect on this process, since the spin degeneracy was already lifted by the reflection on the normal-metal/ferromagnet interface. Compared to the SOC=0 case, the main difference is the splitting of the interface states at the Nb/Au interface; however, the impact of this effect on the order parameter appears to be negligible.

By solving self-consistently the DBdG equations (assuming again the experimental bulk electron-phonon coupling in the Nb layers, and zero elsewhere) we found an oscillating behavior of the order parameter as shown in Fig. 5. The period of these oscillations depends on the number of Au overlayers since the band structure and the number of quantum-well states depends on the thickness of the Au. The order parameter was calculated as a function of the number of Au overlayers up to 42 layers in two cases: with 12 and 24 Fe layers, and the period of the oscillations has been obtained and plotted in both cases in Fig. 6. For thicker Au overlayers as the number of the quantum-well states are increasing, the bands in the spin-up and spin-down channels are separated by smaller and smaller $\vec{q}$ vectors. Therefore the Cooper pairs may acquire smaller and smaller finite momentum, which leads to an increase of the period of oscillation as a function of the Au thickness as observed in Fig. 6. Our theoretical finding explains the oscillating behavior of the order parameter found in Ref. [33]. The order parameter in the Au enters the boundary conditions for superconductivity, hence it influences the T_c as well. Yamazaki *et al.* [6,7] also found oscillations in the critical temperatue with a period of nine layers. Our results suggest that these T_c oscillations observed in that experiment may also

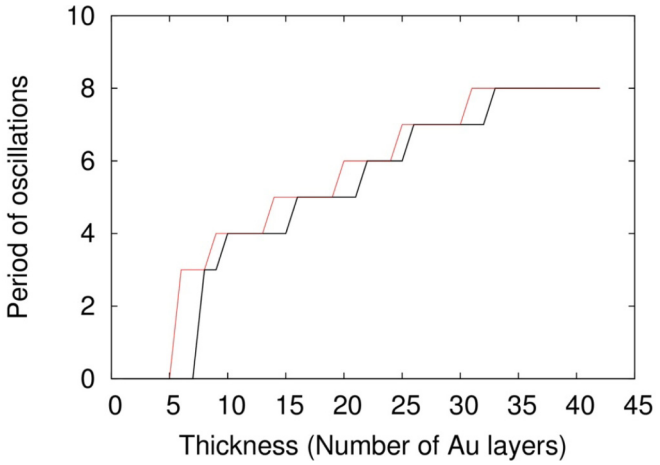

FIG. 6. The oscillations' period of the order parameter as a function of the number of gold overlayers in the case of 12 Fe (black line) and 24 Fe (red line) layers.

be a consequence of the interplay between the quantum-well states and ferromagnetism. We mention that T_c oscillations due to quantum-well states were also reported for Pb thin films in Ref. [57]. The inclusion of more and more Au layers leads to more and more damped oscillations in the Fe layers similarly as was found in Ref. [58].

IV. SUMMARY

In this paper we generalized the screened-KKR method for the solution of the first-principles Dirac–Bogoliubov–de Gennes equations combined with a semiphenomenological parametrization of the exchange-correlation functional. The right-hand-side and left-hand-side solutions corresponding to the single-site problem were derived together with simple conditions when they must be treated separately. As an application of the theory, the order parameters of the Nb/Fe and Nb/Au/Fe systems were obtained. FFLO-type oscillations were found in the Fe layers, but interestingly an oscillatory behavior was also observed in the Au layers. Recent experiments [33] also suggested the existence of similar oscillations in the order parameter (in the Au layers). Based on the results of the band-structure calculations, we could conclude that this is the consequence of the interplay between the quantum-well states and ferromagnetism. We did not investigate the effect of inhomogeneous magnetization, possible triplet correlations, and odd-frequency pairing states which needs further research.

ACKNOWLEDGMENTS

The above work was supported by the Hungarian National Research, Development and Innovation Office under Contracts No. PD124380, No. K115632, and No. K108676; DFG via SFB 689 Spinmomente in reduzierten Dimensionen; and EPSRC through the project "Unconventional Superconductors: New paradigms for new materials" under EP/P007392/1. G.C. acknowledges financial support through a program funded by the German foreign exchange server (DAAD). The authors would like to thank László Szunyogh for fruitful discussions.

[1] P. Fulde and R. A. Ferrell, Phys. Rev. **135**, A550 (1964).
[2] A. I. Larkin and Y. N. Ovchinnikov, Zh. Eksp. Teor. Fiz. **47**, 1136 (1964) [Sov. Phys. JETP **20**, 762 (1965)].
[3] E. A. Demler, G. B. Arnold, and M. R. Beasley, Phys. Rev. B **55**, 15174 (1997).
[4] V. V. Ryazanov, V. A. Oboznov, A. Y. Rusanov, A. V. Veretennikov, A. A. Golubov, and J. Aarts, Phys. Rev. Lett. **86**, 2427 (2001).
[5] A. I. Buzdin, Rev. Mod. Phys. **77**, 935 (2005).
[6] H. Yamazaki, N. Shannon, and H. Takagi, Phys. Rev. B **73**, 094507 (2006).
[7] H. Yamazaki, N. Shannon, and H. Takagi, Phys. Rev. B **81**, 094503 (2010).
[8] J. F. Annett, Adv. Phys. **39**, 83 (1990).
[9] M. Sigrist and K. Ueda, Rev. Mod. Phys. **63**, 239 (1991).
[10] J. Quintanilla, A. D. Hillier, J. F. Annett, and R. Cywinski, Phys. Rev. B **82**, 174511 (2010).
[11] *Non-Centrosymmetric Superconductors: Introduction and Overview*, edited by E. Bauer and M. Sigrist (Springer, Berlin/Heidelberg, 2012).
[12] M. Smidman, M. B. Salamon, H. Q. Yuan, and D. F. Agterberg, Rep. Prog. Phys. **80**, 036501 (2017).
[13] F. S. Bergeret and I. V. Tokatly, Phys. Rev. Lett. **110**, 117003 (2013).
[14] X. Liu, J. K. Jain, and C.-X. Liu, Phys. Rev. Lett. **113**, 227002 (2014).
[15] F. S. Bergeret and I. V. Tokatly, Phys. Rev. B **89**, 134517 (2014).
[16] S. H. Jacobsen and J. Linder, Phys. Rev. B **92**, 024501 (2015).
[17] C. R. Reeg and D. L. Maslov, Phys. Rev. B **92**, 134512 (2015).
[18] J. Alicea, Rep. Prog. Phys. **75**, 076501 (2012).
[19] P. G. de Gennes, *Superconductivity of Metals and Alloys* (W. A. Benjamin, New York, 1966).
[20] K. Capelle and E. K. U. Gross, Phys. Rev. B **59**, 7140 (1999).
[21] K. Capelle and E. K. U. Gross, Phys. Rev. B **59**, 7155 (1999).
[22] J. S. Faulkner, Phys. Rev. B **19**, 6186 (1979).
[23] J. S. Faulkner and G. M. Stocks, Phys. Rev. B **21**, 3222 (1980).
[24] A. Gonis, Phys. Rev. B **33**, 5914 (1986).
[25] L. Szunyogh, B. Újfalussy, P. Weinberger, and J. Kollár, Phys. Rev. B **49**, 2721 (1994).
[26] R. Zeller, P. H. Dederichs, B. Újfalussy, L. Szunyogh, and P. Weinberger, Phys. Rev. B **52**, 8807 (1995).
[27] P. Strange, H. Ebert, J. B. Staunton, and B. L. Gyorffy, J. Phys.: Condens. Matter **1**, 2959 (1989).
[28] E. Tamura, Phys. Rev. B **45**, 3271 (1992).
[29] T. Huhne, C. Zecha, H. Ebert, P. H. Dederichs, and R. Zeller, Phys. Rev. B **58**, 10236 (1998).
[30] H. Ebert, D. Ködderitzsch, and J. Minár, Rep. Prog. Phys. **74**, 096501 (2011).
[31] H. Ebert, J. Braun, D. Ködderitzsch, and S. Mankovsky, Phys. Rev. B **93**, 075145 (2016).
[32] G. Csire, B. Újfalussy, J. Cserti, and B. Gyorffy, Phys. Rev. B **91**, 165142 (2015).

[33] H. Yamazaki, M. Kubota, N. Miyata, and M. Takeda, RIKEN Accel. Prog. Rep. **48**, 253 (2015).
[34] M. B. Suvasini, W. M. Temmerman, and B. L. Gyorffy, Phys. Rev. B **48**, 1202 (1993).
[35] G. Csire, S. Schönecker, and B. Újfalussy, Phys. Rev. B **94**, 140502(R) (2016).
[36] A. Linscheid, A. Sanna, F. Essenberger, and E. K. U. Gross, Phys. Rev. B **92**, 024505 (2015).
[37] A. Linscheid, A. Sanna, and E. K. U. Gross, Phys. Rev. B **92**, 024506 (2015).
[38] M. A. L. Marques, M. Lüders, N. N. Lathiotakis, G. Profeta, A. Floris, L. Fast, A. Continenza, E. K. U. Gross, and S. Massidda, Phys. Rev. B **72**, 024546 (2005).
[39] A. Floris, G. Profeta, N. N. Lathiotakis, M. Lüders, M. A. L. Marques, C. Franchini, E. K. U. Gross, A. Continenza, and S. Massidda, Phys. Rev. Lett. **94**, 037004 (2005).
[40] A. Floris, A. Sanna, S. Massidda, and E. K. U. Gross, Phys. Rev. B **75**, 054508 (2007).
[41] C. Bersier, A. Floris, P. Cudazzo, G. Profeta, A. Sanna, F. Bernardini, M. Monni, S. Pittalis, S. Sharma, H. Glawe, A. Continenza, S. Massidda, and E. K. U. Gross, J. Phys.: Condens. Matter **21**, 164209 (2009).
[42] S. Massidda, F. Bernardini, C. Bersier, A. Continenza, P. Cudazzo, A. Floris, H. Glawe, M. Monni, S. Pittalis, G. Profeta, A. Sanna, S. Sharma, and E. K. U. Gross, Supercond. Sci. Technol. **22**, 034006 (2009).
[43] A. Sanna, G. Profeta, S. Massidda, and E. K. U. Gross, Phys. Rev. B **86**, 014507 (2012).
[44] J. A. Flores-Livas, M. Amsler, C. Heil, A. Sanna, L. Boeri, G. Profeta, C. Wolverton, S. Goedecker, and E. K. U. Gross, Phys. Rev. B **93**, 020508 (2016).
[45] A. J. Flores-Livas, A. Sanna, and K. E. Gross, Eur. Phys. J. B **89**, 1 (2016).
[46] G. Csire, J. Cserti, and B. Újfalussy, J. Phys.: Condens. Matter **28**, 495701 (2016).
[47] J. Zabloudil, R. Hammerling, L. Szunyogh, and P. Weinberger, *Electron Scattering in Solid Matter: A Theoretical and Computational Treatise*, Springer Series in Solid-State Sciences Vol. 147 (Springer, New York, 2005).
[48] B. L. Gyorffy, Z. Szotek, W. M. Temmerman, O. K. Andersen, and O. Jepsen, Phys. Rev. B **58**, 1025 (1998).
[49] H. Ebert, H. Freyer, A. Vernes, and G.-Y. Guo, Phys. Rev. B **53**, 7721 (1996).
[50] K. Kawaguchi and M. Sohma, Phys. Rev. B **46**, 14722 (1992).
[51] G. Verbanck, C. D. Potter, V. Metlushko, R. Schad, V. V. Moshchalkov, and Y. Bruynseraede, Phys. Rev. B **57**, 6029 (1998).
[52] T. Mühge, K. Theis-Bröhl, K. Westerholt, H. Zabel, N. N. Garif'yanov, Y. V. Goryunov, I. A. Garifullin, and G. G. Khaliullin, Phys. Rev. B **57**, 5071 (1998).
[53] A. V. Pronin, M. Dressel, A. Pimenov, A. Loidl, I. V. Roshchin, and L. H. Greene, Phys. Rev. B **57**, 14416 (1998).
[54] B. J. Powell, J. F. Annett, and B. L. Györffy, J. Phys. A **36**, 9289 (2003).
[55] T. Kontos, M. Aprili, J. Lesueur, and X. Grison, Phys. Rev. Lett. **86**, 304 (2001).
[56] Y. V. Fominov, N. M. Chtchelkatchev, and A. A. Golubov, J. Exp. Theor. Phys. Lett. **74**, 96 (2001).
[57] Y. Chen, A. A. Shanenko, and F. M. Peeters, Phys. Rev. B **85**, 224517 (2012).
[58] M. Krawiec, J. Annett, and B. Györffy, Acta Phys. Pol. A **109**, 507 (2006).